

Cavity-Controlled High Harmonic Generation

Zohar Amitay^{1,*} and Nimrod Moiseyev^{1,2,†}

¹*Schulich Faculty of Chemistry and Institute of Advanced Studies in Theoretical Chemistry,
Technion-Israel Institute of Technology, Haifa 32000, Israel*

²*Faculty of Physics, Technion-Israel Institute of Technology, Haifa 32000, Israel*

Employing non-Hermitian Floquet theory, the strong-field process of high harmonic (HH) generation by a classical continuous-wave field irradiating ground-state atom is discovered to be controllable by placing the irradiated atom inside a single-mode quantum cavity initiated even with a single photon. Judicious cavity coupling of cavity-free photo-induced atomic Floquet states forms polaritonic Floquet states that generate side harmonics around the (standard no-cavity) odd harmonics. The different possible cavity-controlled HH spectra, including also the ones resulting from several cavities in a row, enable attosecond-pulse sequences different from the one produced without a cavity. Moreover, the present study sets the framework and opens the way for further cavity control over the HH generation process as well as over other strong-field processes

As recognized in the 2023 Nobel Prize [1, 2], the celebrated process of high harmonic generation (HHG) [3–12] by a strong classical field is a nonlinear strong-field optical process of high scientific interest and importance, both on its own and as a basis for attosecond pulse generation and XUV spectroscopy. In the basic continuous-wave (cw) HHG process with atoms, the irradiation of a ground-state atom with a linearly-polarized strong cw field of frequency ω_0 photo-induces the emission of coherent radiation with frequencies that are high harmonics of ω_0 . With an infrared (IR) driving field, the emitted radiation can extend into the extreme ultraviolet (XUV) region and x-ray region. A key characteristic and limitation of this HHG process is the emission of high-harmonic (HH) radiation only at odd harmonics of ω_0 .

Here, employing non-Hermitian Floquet theory, we discover the process of HHG by a cw classical field irradiating ground-state atoms to be controllable by placing the irradiated atom inside a single-mode quantum cavity that is initiated even with a single photon. Judicious cavity coupling of cavity-free atomic Floquet states (solutions), which are photo-induced by the strong classical cw field, forms polaritonic Floquet states that, once populated, generate side harmonics around the (standard no-cavity) odd harmonics. The specific HH spectrum that is generated depends on the combined properties of the whole atom-cw field-cavity system, i.e., on the specific atomic system, the frequency and intensity of the irradiating cw field, and the cavity frequency and cavity-atom coupling strength. The different possible cavity-controlled HH spectra, including also the ones resulting from several cavities in a row, enable the production of attosecond-pulse sequences that are different from the one produced without a cavity.

To set the theoretical framework, we start with a cavity-free high harmonic generation, where a Xe atom, chosen as the present atomic model system, is irradiated by a strong classical linearly-polarized continuous-wave (cw) field of amplitude ε_0 and frequency ω_0 . The field propagates along the z direction and its linear polariza-

tion is in the x direction. In the length gauge and under the dipole approximation, the time-dependent Hamiltonian of the irradiated atom is given by

$$\hat{H}(x, t) = \hat{H}_{atom}(x) + \hat{d} \varepsilon_0 \cos(\omega_0 t), \quad (1)$$

where $\hat{H}_{atom}(x)$ is the field-free Hamiltonian of the Xe atom, which is taken here as a one-dimensional single-active-electron model Hamiltonian of coordinate x [13] (along the direction of the field's polarization), and $\hat{d} = -ex$ is the corresponding atomic dipole-moment operator ($-e$ is the electron charge).

Within the non-Hermitian quantum Floquet theory [14], following complex scaling of the atomic coordinate x , the time-dependent solution of the time-dependent Schrödinger equation of the irradiated atom with the complex-scaled non-Hermitian Hamiltonian is generally given by

$$|\Psi(x, t)\rangle = \sum_{\alpha} a_{\alpha} |\chi_{\alpha}(x, t)\rangle, \quad (2)$$

with

$$|\chi_{\alpha}(x, t)\rangle = \exp(-i\epsilon_{\alpha}t/\hbar) |\Phi_{\alpha}(x, t)\rangle, \quad (3)$$

where a_{α} , $|\Phi_{\alpha}(x, t)\rangle$ and $\epsilon_{\alpha} = E_{\alpha} - i\Gamma_{\alpha}/2$ are, respectively, the amplitude, eigenfunction and complex eigenenergy (quasienergy) of a resonance Floquet eigenstate α . The E_{α} and $-\Gamma_{\alpha}/2$ are, respectively, the real and imaginary parts of the quasienergy ϵ_{α} , with E_{α} and Γ_{α} being, respectively, the resonance energetic position and width. The amplitudes a_{α} are determined by the initial state of the system at $t=0$. The Floquet eigenstate α is an eigenstate of the complex-scaled non-Hermitian Floquet Hamiltonian $\hat{H}_f(x_{\theta}, t)$ defined as

$$\hat{H}_f(x_{\theta}, t) = -i\hbar \frac{\partial}{\partial t} + \hat{H}_{atom}(x_{\theta}) + \hat{d}_{\theta} \varepsilon_0 \cos(\omega_0 t), \quad (4)$$

such that

$$\hat{H}_f(x_{\theta}, t) |\Phi_{\alpha}^{\theta}(x, t)\rangle = (E_{\alpha} - i\Gamma_{\alpha}/2) |\Phi_{\alpha}^{\theta}(x, t)\rangle, \quad (5)$$

where $x_\theta = x \exp(i\theta)$ is the complex-scaled atomic coordinate replacing x , and $\hat{d}_\theta = -ex_\theta$ is the complex-scaled dipole operator, with θ being the complex-scaling parameter set to a proper value [14]. It is worth noting that each Floquet eigenfunction $|\Phi_\alpha^\theta(x, t)\rangle$ satisfies outgoing spatial boundary conditions, is square integrable with a normalization to one under c -product, and is orthogonal under c -product to all the other Floquet eigenfunctions [14]. For simplicity, from now on we omit the symbol θ .

The Floquet eigenfunctions are time periodic with the cw-field optical period $T_0 = 2\pi/\omega_0$, and each of them is thus given by

$$|\Phi_\alpha(x, t)\rangle = |\Phi_\alpha(x, t + T_0)\rangle = \sum_{n=-\infty}^{\infty} \exp(in\omega_0 t) |\varphi_{n,\alpha}(x)\rangle. \quad (6)$$

where the Fourier component $|\varphi_{n,\alpha}(x)\rangle$ is referred to as the n -th channel function of Floquet eigenstate α . Since $|\varphi_{n,\alpha}(x)\rangle$ can be expanded in the basis set of the field-free atomic eigenstates, $|\Phi_\alpha(x, t)\rangle$ is therefore a complicated time-dependent coherent superposition of them.

With the present Floquet Hamiltonian of Eq. (4), another important characteristic existing here for a given Floquet eigenfunction is its spatio-temporal dynamical symmetry [14, 15],

$$|\Phi_\alpha(x, t)\rangle = S_\alpha |\Phi_\alpha(-x, t + T_0/2)\rangle \quad \text{with } S_\alpha = (+) \text{ or } (-). \quad (7)$$

This implies that all its channel functions possess the symmetry property

$$\varphi_{n,\alpha}(x) = S_\alpha (-1)^n \varphi_{n,\alpha}(-x) \quad (8)$$

according to the Floquet-state category, that is: (i) for a Floquet eigenstate of $S_\alpha = (+)$, $\varphi_{n,\alpha}(x) = \mp \varphi_{n,\alpha}(-x)$ for odd and even n , respectively; whereas (ii) for a Floquet eigenstate of $S_\alpha = (-)$, $\varphi_{n,\alpha}(x) = \pm \varphi_{n,\alpha}(-x)$ for odd and even n , respectively.

The temporal amplitude of the emitted (HH) field is proportional to the time-dependent electron acceleration [8, 13, 15]. Hence, when the system populates a single given Floquet eigenstate α , it is obtained from

$$a_\alpha^{\text{HH}}(t) = \frac{\partial^2}{\partial t^2} (\chi_\alpha(x, t) | x | \chi_\alpha(x, t)) . \quad (9)$$

Following Fourier transform, the resulting relative amplitude of the high-harmonic field generated at frequency $\Omega = M\omega_0$, with M being an integer (for simplicity), is then given by [8, 13]

$$A_\alpha^{\text{HH}}(M\omega_0) = -(M\omega_0)^2 \sum_{n=-\infty}^{\infty} (\varphi_{n+M,\alpha}(x) | x | \varphi_{n,\alpha}(x))_x , \quad (10)$$

i.e., it results from a summation over all the dipole matrix elements between pairs of Floquet channel functions of eigenstate α whose orders differ by the harmonic order

M . The corresponding high-harmonic spectral intensity is then

$$I_\alpha^{\text{HH}}(M\omega_0) = |A_\alpha^{\text{HH}}(M\omega_0)|^2 . \quad (11)$$

Following Eqs. (7)–(11), symmetry considerations directly imply that $A_\alpha^{\text{HH}}(M\omega_0)$ and $I_\alpha^{\text{HH}}(M\omega_0)$ are generally nonzero for odd M and zero for even M , i.e., only odd high harmonics are generated when a single Floquet eigenstate is populated [8, 13, 15]. It applies to both the so-called plateau and cutoff regions of the HH spectrum.

Next, we consider a cavity-free system of a Xe atom that initially populates its field-free ground (electronic) state and is then irradiated by a strong cw field having an amplitude of up to about $\varepsilon_0 = 0.4$ (atomic units). As previously shown [8], this system predominantly populates the Floquet eigenstate $\alpha = FLg$ that its eigenfunction $|FLg\rangle = |\Phi_{FLg}(x, t)\rangle$ has the largest spatial overlap with the the eigenfunction of the field-free ground state of Xe among all the system's Floquet eigenfunctions. This largest overlap is of value close to 1. Hence, as presented above, only odd high harmonics are generated during such cw irradiation of Xe. This is the non-Hermitian Floquet quantum-mechanical explanation for this well-known phenomenon of odd-only HHG by ground-state atoms irradiated by a cw field [3–5, 8, 13, 15]. Fig. 2(b1) shows the corresponding cavity-free theoretical results of the odd-only HH spectrum calculated for the model ground-state Xe atom irradiated by a cw field of amplitude $\varepsilon = 0.04$, corresponding to an intensity of 5×10^{13} W/cm², and of frequency $\omega_0 = 0.057$, corresponding to a wavelength of 800 nm. Throughout this paper, the units of quantities written as unitless are atomic units.

Following the well-established framework described above, we move now to the innovative part of the study, presenting the cavity-controlled HHG. Here, the previously described system—an irradiated Xe atom initially in its field-free ground state and then in the cavity-free Floquet eigenstate FLg (see above)—is placed within a single-mode quantum cavity that is initially seeded with a single photon. Fig. 1(a1) schematically shows the corresponding scheme. As considered earlier, a strong classical cw field with amplitude ε_0 and frequency ω_0 , linearly polarized along the x direction and propagating along the z direction, irradiates the model Xe atom having its atomic coordinate x along the x direction. In addition, the newly introduced cavity of frequency ω_{cav} has its axis along the y direction, and its single-mode field considered here is also linearly polarized along the x direction. This configuration ensures, for clarity and simplicity, that the photonic modes of the cavity and of the strong cw field are different. Additionally, for simplicity, to avoid the possibility of any emitted high-harmonic radiation being trapped in the cavity, ω_{cav} is assumed to be a non-integer multiple of ω_0 .

The Hamiltonian \hat{H}_{cav} describing this whole system of the irradiated Xe atom in a cavity is then given by the cavity-free \hat{H} [Eq.(1)] with the addition of time-independent cavity-dependent terms,

$$\hat{H}_{cav} = \hat{H}(x, t) + \hbar\omega_{cav} \hat{a}_{cav}^\dagger \hat{a}_{cav} + \hat{d} \varepsilon_{cav} (\hat{a}_{cav}^\dagger + \hat{a}_{cav}), \quad (12)$$

where \hat{a}_{cav}^\dagger and \hat{a}_{cav} are the creation and annihilation operators of the cavity mode, respectively. The quantity $\varepsilon_{cav} \equiv \sqrt{(\hbar\omega_{cav}) / (2\bar{\epsilon}_0 V)}$ is the cavity-atom coupling strength parameter, with V being the cavity (quantization) volume and $\bar{\epsilon}_0$ being the vacuum permittivity. The dipole self-energy term $[\varepsilon_{cav}^2 \hat{d}_\theta^2 / (\hbar\omega_{cav})]$ has been omitted from \hat{H}_{cav} . The corresponding non-Hermitian Floquet Hamiltonian $\hat{H}_{cav,f}$ is then given by the cavity-free \hat{H}_f [Eq.(4)] with the addition of the corresponding cavity-dependent terms,

$$\hat{H}_{cav,f} = \hat{H}_f(x, t) + \hbar\omega_{cav} \hat{a}_{cav}^\dagger \hat{a}_{cav} + \hat{d}_\theta \varepsilon_{cav} (\hat{a}_{cav}^\dagger + \hat{a}_{cav}). \quad (13)$$

The eigenstates of $\hat{H}_{cav,f}$ are Floquet eigenstates that simultaneously describe the irradiated Xe atom and the cavity field; we therefore term them polaritonic Floquet eigenstates (Floquet polaritons). The initial (polaritonic) state of the system—here, an irradiated Xe atom in FLg , and a cavity with a single photon—determines their amplitudes. This, in turn, dictates the time-dependent wavefunction of the system and the emitted HH field. Overall, the generated HH spectrum is determined and controlled by the complete set of properties of the different system components—i.e., the atom, the strong cw field, and the cavity—as well as by the initial state of the system.

In analogy to the Jaynes-Cummings model [16], for studying the essence of cavity-controlled HHG, we consider here a model that includes only a pair of cavity-free Floquet eigenstates of the irradiated Xe atom. Specifically, they are chosen as the cavity-free Floquet eigenstates $\alpha=FLg$ and $\alpha=FLe$ that have the largest spatial overlap, among all the cavity-free Floquet eigenstates, with the field-free ground and first-excited states of Xe, respectively. The real parts of their quasienergies, ϵ_{FLg} and ϵ_{FLe} , satisfy $E_{FLg} < E_{FLe}$. As described before, the initial (polaritonic) wavefunction of the system is

$$|\Psi_{cav}(t=0)\rangle = |FLg, 1\rangle = |\Phi_{FLg}(x, t)\rangle |1\rangle_{cav}, \quad (14)$$

where $|n_{ph}\rangle_{cav}$ is the photonic eigenstate (QED number state) of the cavity mode with n_{ph} photons and no atom in the cavity. The present study is conducted under the Rotating-Wave Approximation. Therefore, following this $\Psi_{cav}(t=0)$, the system and its dynamics are fully described within the "single-excitation" polaritonic

subspace spanned by the two basis functions

$$\begin{aligned} |FLg, 1\rangle &= |\Phi_{FLg}(x, t)\rangle |1\rangle_{cav} \\ |FLe, 0\rangle &= |\Phi_{FLe}(x, t)\rangle |0\rangle_{cav}, \end{aligned}$$

which correspond to the irradiated Xe atom in either FLg or FLe , with the cavity mode containing one or zero photons, respectively.

Hence, $\hat{H}_{cav,f}$ is given by the following 2×2 matrix representation:

$$\begin{aligned} [\hat{H}_{cav,f}]_{11} &= \langle FLg, 1 | \hat{H}_{cav,f} | FLg, 1 \rangle = \\ &= \epsilon_{FLg} + \hbar\omega_{cav} = (E_{FLg} - i\Gamma_{FLg}/2) + \hbar\omega_{cav}, \end{aligned}$$

$$\begin{aligned} [\hat{H}_{cav,f}]_{22} &= \langle FLe, 0 | \hat{H}_{cav,f} | FLe, 0 \rangle = \\ &= \epsilon_{FLe} = (E_{FLe} - i\Gamma_{FLe}/2), \end{aligned}$$

$$\begin{aligned} [\hat{H}_{cav,f}]_{12} &= \langle FLg, 1 | \hat{H}_{cav,f} | FLe, 0 \rangle = \\ &= \varepsilon_{cav} d_{FLe, FLg} = \varepsilon_{cav} \sum_{n=-\infty}^{\infty} (\varphi_{n, FLe}(x) | x | \varphi_{n, FLg}(x))_x, \end{aligned}$$

$$\begin{aligned} [\hat{H}_{cav,f}]_{21} &= \langle FLe, 0 | \hat{H}_{cav,f} | FLg, 1 \rangle = \\ &= \varepsilon_{cav} d_{FLg, FLe} = \varepsilon_{cav} \sum_{n=-\infty}^{\infty} (\varphi_{n, FLg}(x) | x | \varphi_{n, FLe}(x))_x. \end{aligned}$$

Following Eqs. (7)–(8), the non-diagonal terms, $[\hat{H}_{cav,f}]_{12}$ and $[\hat{H}_{cav,f}]_{21}$, are non-zero only when FLg and FLe differ in their dynamical symmetry; as analyzed below, only in such a case does the cavity have any influence on the HHG. The polaritonic Floquet eigenstates of the system within the single-excitation subspace, i.e., the upper and lower Floquet polaritons, are then given as the eigenstates of $\hat{H}_{cav,f}$,

$$\hat{H}_{cav,f} \left| \Phi_{cav, \pm}^{(\omega_{cav}, \varepsilon_{cav})} \right\rangle = \epsilon_{cav, \pm}^{(\omega_{cav}, \varepsilon_{cav})} \left| \Phi_{cav, \pm}^{(\omega_{cav}, \varepsilon_{cav})} \right\rangle, \quad (15)$$

with their (complex) eigenenergies being

$$\epsilon_{cav, \pm}^{(\omega_{cav}, \varepsilon_{cav})} = \frac{1}{2} (\epsilon_{FLg} + \hbar\omega_{cav} + \epsilon_{FLe}) \pm \frac{1}{2} \hbar\Omega, \quad (16)$$

and their eigenfunctions being

$$\left| \Phi_{cav, \pm}^{(\omega_{cav}, \varepsilon_{cav})} \right\rangle = \sqrt{\frac{\Omega \pm \delta}{2\Omega}} |FLg, 1\rangle \pm \sqrt{\frac{\Omega \mp \delta}{2\Omega}} |FLe, 0\rangle, \quad (17)$$

where

$$\begin{aligned}
\hbar \Omega &= \sqrt{(\hbar \delta)^2 + (\hbar \Omega_0)^2}, \\
\hbar \delta &= \epsilon_{FLg} + \hbar \omega_{cav} - \epsilon_{FLe}, \\
\hbar \Omega_0 &= 2 \epsilon_{cav} d_{FLg, FLe} = \\
&= 2 \epsilon_{cav} \sum_{n=-\infty}^{\infty} (\varphi_{n, FLe}(x) | x | \varphi_{n, FLg}(x))_x, \quad (18)
\end{aligned}$$

with Ω_0 being the system's (complex) Rabi frequency.

With these upper and lower Floquet polaritons, the time-dependent wavefunction of the system evolves from its initial state $\Psi_{cav}(t=0)=|FLg, 1\rangle$ as their coherent superposition:

$$\begin{aligned}
|\Psi_{cav}(t)\rangle &= \\
&= a_{cav,+} \exp\left(-i\epsilon_{cav,+}^{(\omega_{cav}, \epsilon_{cav})} t/\hbar\right) |\Phi_{cav,+}^{(\omega_{cav}, \epsilon_{cav})}\rangle + \\
&\quad a_{cav,-} \exp\left(-i\epsilon_{cav,-}^{(\omega_{cav}, \epsilon_{cav})} t/\hbar\right) |\Phi_{cav,-}^{(\omega_{cav}, \epsilon_{cav})}\rangle, \\
a_{cav,\pm} &= \sqrt{\frac{\Omega \pm \delta}{2\Omega}}. \quad (19)
\end{aligned}$$

The generated HH field is then given by

$$a_{cav}^{HH}(t) = \frac{\partial^2}{\partial t^2} (\Psi_{cav}(t) | x | \Psi_{cav}(t)) . \quad (20)$$

Using Eq. (19), the right-hand side of Eq. (20) contains terms that involve either $\Phi_{cav,+}^{(\omega_{cav}, \epsilon_{cav})}$ or $\Phi_{cav,-}^{(\omega_{cav}, \epsilon_{cav})}$ alone (see Eq. (17)), and others that involve both. Following Fourier transform, these two groups of terms generally give rise to different parts of the resulting cavity-controlled HH spectrum: the former yields odd harmonics, which also exist in the no-cavity case, whereas the latter generates side harmonics around these odd harmonics, which do not appear without the cavity. The respective HH field amplitudes at frequencies $\Omega = M\omega_0$ and $\Omega = (M \pm \Delta M)\omega_0$, with M being an integer, are obtained to be

$$\begin{aligned}
A_{cav}^{HH}(M\omega_0) &= \\
&= \left(\frac{\Omega^2 + \delta^2}{2\Omega^2}\right) A_{FLg}^{HH}(M\omega_0) + \left(\frac{\Omega^2 - \delta^2}{2\Omega^2}\right) A_{FLe}^{HH}(M\omega_0), \quad (21)
\end{aligned}$$

and

$$\begin{aligned}
A_{cav}^{HH}((M \pm \Delta M)\omega_0) &= \\
&= \kappa \left(\frac{\Omega^2 - \delta^2}{4\Omega^2}\right) (A_{FLg}^{HH}(M\omega_0) - A_{FLe}^{HH}(M\omega_0)), \\
\Delta M &= \left(\epsilon_{cav,+}^{(\omega_{cav}, \epsilon_{cav})} - \epsilon_{cav,-}^{(\omega_{cav}, \epsilon_{cav})}\right) / (\hbar \omega_0), \\
\kappa &= \left(\frac{M \pm \Delta M}{M}\right)^2, \quad (22)
\end{aligned}$$

where $A_{FLg}^{HH}(M\omega_0)$ and $A_{FLe}^{HH}(M\omega_0)$ are the cavity-free high-harmonic field amplitudes generated at frequency $\Omega = M\omega_0$ when the irradiated Xe atom populates solely FLg or FLe , respectively (see Eq. (10)). The HH amplitude generated in the cavity at frequency Ω is then generally given by

$$\begin{aligned}
A_{cav}^{HH}(\Omega) &= \delta_{\Omega, M\omega_0} A_{cav}^{HH}(M\omega_0) + \\
&\quad \delta_{\Omega, (M \pm \Delta M)\omega_0} A_{cav}^{HH}((M \pm \Delta M)\omega_0), \quad (23)
\end{aligned}$$

with the corresponding HH spectral intensity being

$$I_{cav}^{HH}(\Omega) = |A_{cav}^{HH}(\Omega)|^2. \quad (24)$$

As seen, for a given atomic system and strong cw field, the cavity parameters ω_{cav} and ϵ_{cav} determine the shift parameter ΔM , which sets the displacement of the side harmonics at frequencies $(M \pm \Delta M)\omega_0$ relative to the odd harmonic at frequency $M\omega_0$.

Following the above, the cavity control over the generated HH spectrum can be further enhanced by extending the basic scheme of a single irradiated Xe atom in a single cavity to an arrangement of several (N_{cav}) cavities placed in a row, each containing one irradiated Xe atom. Each Xe atom is initially in its field-free ground electronic state, and each cavity is seeded with a single photon. The strong cw field passes through the sequence of cavities, accompanied by the HH fields generated in all preceding cavities, which coherently add together. As an example, the case of two cavities in a row is schematically illustrated in Fig. 1(a2). With each of the N_{cav} cavities generally having a different pair of values for ω_{cav} and ϵ_{cav} that corresponds to a different shift parameter ΔM (i.e., cavity i produces side harmonics with a shift of ΔM_i), the overall HH spectrum contains now a series of side harmonics around each odd harmonic at the shifts $\Delta M_1, \Delta M_2, \dots, \Delta M_{N_{cav}}$.

Figure 2 shows several illustrative examples of the corresponding theoretical results numerically calculated for the cavity-controlled HHG by single irradiated Xe atoms in one or more cavities. Each of the cavities is initially

seeded with a single photon. Each of the Xe atoms is initially in its field-free ground state, and is irradiated by a strong linearly-polarized cw field having a frequency of $\omega_0=0.057$ (corresponding to a wavelength of 800 nm) and an amplitude of $\varepsilon_0=0.04$ (corresponding to an intensity of 5×10^{13} W/cm²). For the HH yield generated by a single irradiated Xe atom in a single cavity, Fig. 2(a) shows the total HH intensity I_{tot}^{HH} (i.e., after summation over all frequencies) as a function of ε_{cav} for several values of ω_{cav} . Note the logarithmic scale of the y-axis. As seen, there is a very high sensitivity of I_{tot}^{HH} to the cavity parameters, with orders-of-magnitude changes among the different cases, particularly as compared to the no-cavity case. For the HH spectrum generated by a single irradiated Xe atom in a single cavity, Fig. 2(b1) shows the generated HH spectrum for the case of no cavity, and Figs. 2(b2) and 2(b3) show the generated HH spectrum for, respectively, the cases of: (i) $\omega_{cav}=6.45\omega_0$ and $\varepsilon_{cav} = 0.229$, corresponding to a side-harmonic shift of $\Delta M=\pm 1.0$, which means harmonic spacing of ω_0 with the generation of both odd and even harmonics; and (ii) $\omega_{cav}=6.45\omega_0$ and $\varepsilon_{cav} = 0.235$, corresponding to a side-harmonic shift of $\Delta M=\pm 0.5$. Then, going beyond a single cavity, Fig. 2(d1) presents results for the HH spectrum generated by a sequence of two cavities with a single irradiated Xe atom in each. Specifically here, these two cavities are the individual cavities of Figs. 2(b2) and (c2), one corresponding to $\Delta M=\pm 1.0$ while the other to $\Delta M=\pm 0.5$, which means harmonic spacing of $\omega_0/2$ with the generation of odd and even harmonics as well as the middle harmonic between each odd-even pair. Going to an even larger number of cavities, Fig. 2(d2) displays results for the HH spectrum generated by a sequence of ten cavities with a single irradiated Xe atom in each. All the ten cavities have a frequency of $\omega_{cav}=6.45\omega_0$, while their ε_{cav} spans the range of 0.238 to 0.256, corresponding to shift magnitude $|\Delta M|$ of 0.1 to 1.0 in a step of 0.1, which means harmonic spacing of $\omega_0/10$. In general, there is also the possibility of blocking some harmonics in a generated HH spectrum to yield a corresponding modified spectrum. As seen from all the above, in contrast to the HH spectrum generated without a cavity, the cavity-induced spectra include side harmonics around the odd harmonics, exhibit spectral intensities enhanced by orders of magnitude, and extend the plateau and cutoff regions to much higher harmonic orders. Overall, the demonstrated cavity control over the generated HH spectrum is extremely rich.

Since one of the prominent uses of HHG is the production of attosecond pulses [12], Fig. 2 also presents results for the attosecond pulse sequence that can be generated in the different cases. Fig. 2(c1) shows the temporal attosecond pulse sequence generated from the cutoff region (beyond the 26th harmonic, H26) of the no-cavity HH spectrum presented in Fig. 2(b1), after setting all the HH spectral phase to zero, i.e., it is the corresponding

transform-limited (TL) attosecond pulse sequence. As is well known, and seen, the generated attosecond pulses are spaced by $T_0/2$, with T_0 being the optical period of the strong cw field irradiating the Xe atom. Fig. 2(c2) shows the TL attosecond pulse sequence that generated from the cutoff region (beyond H26) of the cavity-induced HH spectrum presented in Fig. 2(b2). Since the harmonic spacing in this spectrum is ω_0 , as seen, the generated attosecond pulses are spaced here by T_0 , which is impossible without the cavity. Similarly, Fig. 2(c3) shows the TL attosecond pulse sequence generated from the cutoff region (beyond H26) of the cavity-induced HH spectrum presented in panel (b3). Here, the generated attosecond pulse sequence is composed of a pulse every $2T_0$ accompanied by two weaker sub-pulses that are shifted from it by about $\pm 0.5T_0$. To further illustrate the richness and control potential also in the production of the attosecond pulse sequence, Fig. 2(c4) shows the TL attosecond pulse sequence generated from the cutoff region (beyond H26) of the cavity-induced HH spectrum presented in Fig. 2(b3), after the odd harmonics are blocked, i.e., the spectrum contains here only the side harmonics with $\Delta M=\pm 0.5$ around each odd harmonic. This brings the HH spectrum to the case of harmonic spacing of ω_0 , with the existing harmonic orders shifted by $\omega_0/2$ as compared to the HH spectrum of Fig. 2(b2). Following this harmonic spacing of ω_0 , the TL attosecond pulse sequence that is generated here has a temporal spacing of T_0 , similar to the case pulse sequence presented in Fig. 2(c2).

In summary, using non-Hermitian Floquet theory, we demonstrated cavity-controlled HHG, where HHG by a cw classical field irradiating a ground-state atom is controllable by placing the irradiated atom inside a single-mode cavity that is initiated even with a single photon. The control is based on cavity coupling of cavity-free atomic Floquet to form polaritonic Floquet states that their population allows to generate side harmonics around the standard no-cavity odd harmonics, which are the only ones generated without a cavity. The different possible cavity-controlled HH spectra, including also the ones resulting from several cavities in a row, enable the production of attosecond-pulse sequences that are different from the one produced without a cavity. The results and degree of cavity control are extremely sensitive to the different characteristics of the system, including the irradiated atom, the strong cw field and the cavity, hence their judicious selection is highly required. In this spirit, the new theoretical framework established here opens avenues for further cavity control of the HHG process as well as other strong-field photo-processes.

* Electronic address: amitayz@technion.ac.il

- [†] Electronic address: nimrod@technion.ac.il; URL: <https://nhqm.net.technion.ac.il/>
- [1] Press release. NobelPrize.org. 3 Oct. 2023. URL: <https://www.nobelprize.org/prizes/physics/2023/press-release/>.
 - [2] Advanced information. Nobel-Prize.org. 3 Oct. 2023. URL: <https://www.nobelprize.org/prizes/physics/2023/advanced-information/>.
 - [3] M. Ferray, A. L’Huillier, X. F. Li, L. A. Lompre, G. Mainfray, and C. Manus, Journal of Physics B: Atomic, Molecular and Optical Physics **21**, L31 (1988).
 - [4] A. L’Huillier, K. J. Schafer, and K. C. Kulander, Journal of Physics B: Atomic, Molecular and Optical Physics **24**, 3315 (1991).
 - [5] J. L. Krause, K. J. Schafer, and K. C. Kulander, Phys. Rev. Lett. **68**, 3535 (1992).
 - [6] P. B. Corkum, Phys. Rev. Lett. **71**, 1994 (1993).
 - [7] M. Lewenstein, P. Balcou, M. Y. Ivanov, A. L’Huillier, and P. B. Corkum, Phys. Rev. A **49**, 2117 (1994).
 - [8] N. Moiseyev and F. Weinhold, Phys. Rev. Lett. **78**, 2100 (1997).
 - [9] P. Antoine, A. L’Huillier, and M. Lewenstein, Phys. Rev. Lett. **77**, 1234 (1996).
 - [10] P. Salières, A. L’Huillier, P. Antoine, and M. Lewenstein (1997), quant-ph/9710060, URL <https://arxiv.org/abs/quant-ph/9710060>.
 - [11] M. Bellini, C. Lyngå, A. Tozzi, M. B. Gaarde, T. W. Hänsch, A. L’Huillier, and C.-G. Wahlström, Phys. Rev. Lett. **81**, 297 (1998).
 - [12] P. M. Paul, E. S. Toma, P. Breger, G. Mullot, F. Augé, P. Balcou, H. G. Muller, and P. Agostini, Science **292**, 1689 (2001).
 - [13] A. Fleischer and N. Moiseyev, Phys. Rev. A **77**, 010102 (2008).
 - [14] N. Moiseyev, *Non-Hermitian quantum mechanics* (Cambridge University Press, 2011).
 - [15] N. Moiseyev and M. Lein, The Journal of Physical Chemistry A **107**, 7181 (2003).
 - [16] E. T. Jaynes and F. W. Cummings, Proceedings of the IEEE **51**, 89 (1963).

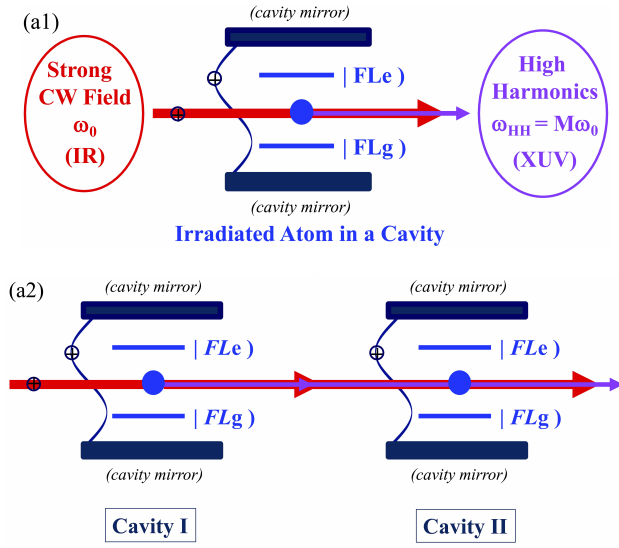


FIG. 1: Schematic of the general scheme for high harmonic generation by individual irradiated atoms in cavities. See text for details.

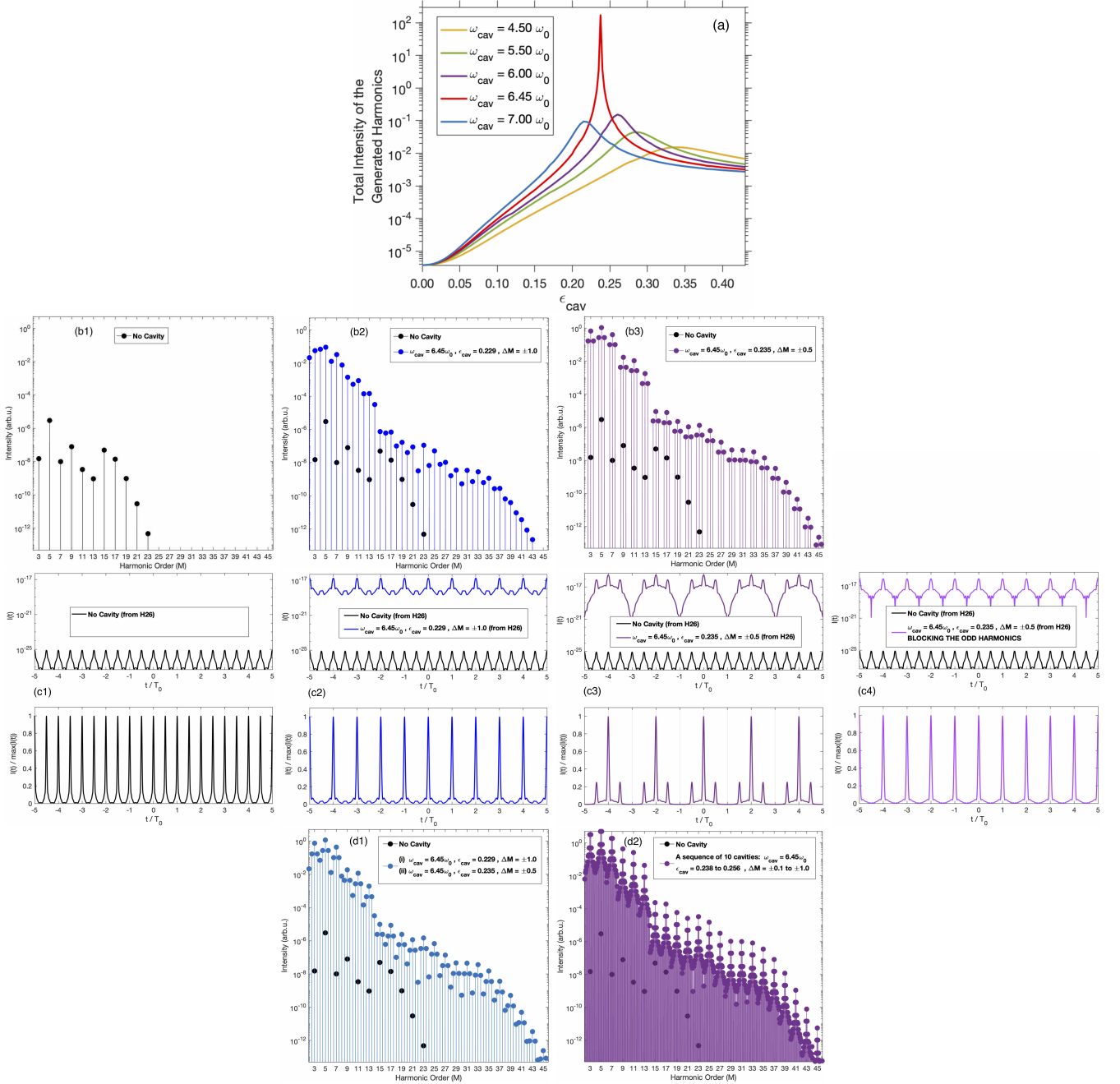


FIG. 2: Examples of the theoretical results numerically calculated for the cavity-controlled HHG by single irradiated Xe atoms in one or more cavities. Each of the cavities is initially seeded with a single photon. Each of the Xe atoms is initially in its field-free ground state, and is irradiated by a strong linearly-polarized cw field having a frequency of $\omega_0=0.057$ (a wavelength of 800 nm) and an amplitude of $\epsilon_0=0.04$ (an intensity of 5×10^{13} W/cm²).

(A) For the HH yield generated by a single irradiated Xe atom in a single cavity: Panel (a) shows the total HH intensity as a function of ϵ_{cav} for several values of ω_{cav} .

(B) For the HH spectrum generated by a single irradiated Xe atom in a single cavity: Panel (b1) shows the generated HH spectrum for the case of no cavity, and panels (b2) and (b3) show the generated HH spectrum for, respectively, the cases of: (i) $\omega_{cav}=6.45\omega_0$ and $\epsilon_{cav} = 0.229$, corresponding to a side-harmonic shift of $\Delta M=\pm 1.0$, and (ii) $\omega_{cav}=6.45\omega_0$ and $\epsilon_{cav} = 0.235$, corresponding to a side-harmonic shift of $\Delta M=\pm 0.5$.

(C) For the attosecond pulse sequence that can be generated in the different HHG cases above: Panel (c1) shows the TL temporal attosecond pulse sequence generated from the cutoff region (beyond the 26th harmonic; H26) of the no-cavity HH spectrum presented in panel (b1), after setting all the HH spectral phase to zero. Panels (c2) and (c3) show the TL attosecond pulse sequence generated from the cutoff region (beyond H26) of the cavity-induced HH spectrum presented in panels (b2) and (b3), respectively. Panel (c4) shows the TL attosecond pulse sequence generated from the cutoff region (beyond H26) of the cavity-induced HH spectrum presented in panel (b3), after the odd harmonics are blocked.

(D) Panel (d1) presents results for the HH spectrum generated by a sequence of two cavities with a single irradiated Xe atom in each. Specifically here, these two cavities are the individual cavities of panels (b2) and (c2), one corresponding to $\Delta M=\pm 1.0$ while the other to $\Delta M=\pm 0.5$. Panel (d2) displays results for the HH spectrum generated by a sequence of ten cavities with a single irradiated Xe atom in each. All the ten cavities have a frequency of $\omega_{cav}=6.45\omega_0$, while their ϵ_{cav} spans the range of 0.238 to 0.256, corresponding to shift magnitude $|\Delta M|$ of 0.1 to 1.0 in a step of 0.1.